Finite-temperature magnetism of Fe_xPd_{1-x} and Co_xPt_{1-x} alloys

S. Polesya,[1] S. Mankovsky,[1] O. Sipr,[2] W. Meindl,[3] C. Strunk,[3] and H. Ebert[1]
[1]*Department of Chemistry, LMU Munich, Butenandtstrasse 11, D-81377 Munich, Germany*
[2]*Institute of Physics AS CR, v. v. i., Cukrovarnicka 10, 162 53 Praha, Czech Republic*
[3]*University Regensburg, D-93040 Regensburg, Germany*
(Received 23 August 2010; published 6 December 2010)

The finite-temperature magnetic properties of Fe_xPd_{1-x} and Co_xPt_{1-x} alloys have been investigated. It is shown that the temperature-dependent magnetic behavior of these alloys cannot be described properly unless the coupling between the magnetic moments at the Fe and Co mediated through the interactions with the induced magnetic moments of the nonmagnetic Pd and Pt atoms is included. A scheme for the calculation of the Curie temperature (T_C) for this type of systems is presented that is based on the extended Heisenberg Hamiltonian with the appropriate exchange parameters J_{ij} obtained from *ab initio* electronic-structure calculations. Within the present study the Korringa-Kohn-Rostoker Green's-function method has been used to calculate the J_{ij} parameters. The Curie temperatures obtained for Fe_xPd_{1-x} and Co_xPt_{1-x} alloys are compared with the corresponding experimental data. The experimental results for Fe_xPd_{1-x} alloys have been obtained within anomalous Hall-effect measurements. The agreement between theoretical results and all available experimental data is rather good.

DOI: 10.1103/PhysRevB.82.214409 PACS number(s): 71.20.Be, 75.30.Hx, 75.40.Cx, 75.40.Mg

I. INTRODUCTION

Whether a magnetic material is technologically useful or not, depends on its properties at finite temperatures. However, the *ab initio* treatment of finite-temperature magnetism remains a challenge despite the ongoing progress in this field during the last decades.

In this context, itinerant-electron 3*d* transition metals and their alloys receive particular interest. For these systems finite-temperature magnetic properties cannot be described successfully neither within the collective-electron Stoner model nor within local-moment models based on the Heisenberg Hamiltonian (for an overview see Refs. 1 and 2). The Stoner model which treats the transition to the paramagnetic state as vanishing of the local magnetic moments, accounting thereby only for the longitudinal spin fluctuations, strongly overestimates the Curie temperature T_C. More success has been achieved using the Heisenberg model which accounts for temperature-induced transverse spin fluctuations and characterizes the paramagnetic state by orientational disorder within the system of localized magnetic moments. However, the magnitude of the moments is assumed to be unchanged upon fluctuations. In some recent studies, the Heisenberg model approach has been combined with *ab initio* band-structure calculations that allow to evaluate the exchange coupling parameters from first principles.[3] In this way, trends of the Curie or Néel temperature with composition can be quantitatively described for many systems, in particular, for transition-metal monoxides,[4] dilute magnetic semiconductors,[5] or transition metals.[6]

Despite the rather satisfying results obtained within this combined approach, the description of finite-temperature magnetism of transition metals and alloys still suffers from various problems because of the restrictions of the Heisenberg model. For some itinerant-electron systems, e.g., Ni, the thermally induced longitudinal spin fluctuations play a crucial role in describing properly the temperature-dependent magnetization and obtaining the correct value for the critical temperature. A phenomenological theory of finite-temperature magnetism which accounts for both types of fluctuations on the same footing was developed in the past.[7–10] This theory was used in combination with *ab initio* electronic-structure calculations to describe temperature-dependent magnetic properties of Fe, Co, and Ni.[11–13] In this way a much better agreement with experiment, as compared to calculations based on the Heisenberg model, was obtained. In particular, proper accounting for longitudinal fluctuations results in the vanishing of local magnetic moments on Ni atoms above T_C (Ref. 13) in agreement with experiment.

Other interesting itinerant-electron systems in this context are alloys or compounds composed of originally magnetic and nonmagnetic elements. Such systems exhibit the so-called covalent magnetism[14,15] where magnetization of the "nonmagnetic" atoms is governed by the spontaneously magnetized atoms via the strong spin-dependent hybridization of their electronic states. The Fe_xPd_{1-x} and Co_xPt_{1-x} alloys considered in the present work belong to this type of systems. To describe the temperature-dependent magnetism of such systems on the basis of Heisenberg model, one obviously has to account properly for the behavior of the Pd/Pt sublattices. Only a few *ab initio* studies of finite-temperature magnetism of such systems have been done so far. Similarly to the work mentioned above[11–13] these studies were based on a generalization of the classical Heisenberg Hamiltonian in one or another way to account for the different character of magnetism on different types of atoms. Mryasov *et al.*[16] have investigated the compound FePt and showed that the anomalous temperature dependence of its magnetocrystalline anisotropy energy is due to the induced Pt magnetic moments. In another study[17] these authors demonstrate a crucial role of the magnetic moment induced on Rh for the stabilization of the ferromagnetic state of FeRh and for the control of the antiferromagnet (AFM)-ferromagnet phase transition. Ležaic *et al.*[18] emphasized the need to account for longitudinal fluctuations of magnetic moments induced on Ni atoms for a

proper description of the temperature dependence of the spin polarization at the Fermi energy E_F in the half-metallic ferromagnet NiMnSb. Sandratskii *et al.*[19] investigated several ways to account for the induced magnetic moments within the spin-spiral approach used for the calculation of the exchange coupling parameters in NiMnSb and MnAs. Using these results Sandratskii *et al.*[19] have studied finite-temperature magnetic properties of NiMnSb; their findings are consistent with the findings of Ležaic *et al.*[18]

In this work we introduce an *ab initio* method to describe finite-temperature magnetism of systems with spontaneous and induced magnetic moments. The method is based on an extension of the Heisenberg Hamiltonian by adding a term which describes the induced magnetic moments within the linear-response formalism. Our approach relies on a combination of *ab initio* band-structure calculations with Monte Carlo (MC) simulations based on the extended Heisenberg model. To test this approach we investigate finite-temperature magnetic properties of Pd-rich Fe_xPd_{1-x} alloys with Fe concentrations up to 20 at. % for which new experimental results are presented. The Fe_xPd_{1-x} system is interesting from the technological point of view. In particular, thin films of these materials are used for contact electrodes in nanoelectronics. Therefore, the magnetic properties of Fe_xPd_{1-x} films have been investigated experimentally in the present work and the results for Curie temperature are compared with theoretical results. We study also ordered and disordered Co_3Pt, CoPt, and $CoPt_3$ alloys as these are interesting both for fundamental reasons and for possible use in industrial applications because of their high magnetic anisotropy.[20,21] Theoretical investigations of finite-temperature magnetism of these systems failed so far to reproduce experimental results with satisfactory accuracy.[22] We demonstrate in the present work that a combination of *ab initio* band-structure calculations with MC simulations based on the extended Heisenberg model gives satisfying agreement between theoretical and experimental values of critical temperatures. We found that despite their small magnitudes the moments induced on nonmagnetic atoms (Pd, Pt) have an important influence on finite-temperature magnetic order.

II. EXPERIMENTAL DETAILS

The present experimental effort has been focused on the investigations of thickness-dependent magnetic properties of these films. Particular interest has their Curie temperature T_C which have drastic deviations from bulk behavior at thicknesses less than $\approx$20 nm.[23,24] However, approaching the film thickness of about 20 nm, their Curie temperature becomes comparable with the corresponding bulk values. This allows to compare T_C measured for Fe_xPd_{1-x} films with theoretical results obtained for bulk Fe_xPd_{1-x} alloys.

The Fe_xPd_{1-x} films were thermally evaporated onto oxidized silicon substrates from separate effusion cells for Pd and Fe in an ultrahigh-vacuum system (base pressure 5×10^{-11} mbar). The film thicknesses were between 15 and 20 nm. The deposition rate of the two components could be controlled independently, resulting in an accuracy of the Fe concentration of 1 at. %. Auger spectroscopy on a sample with nominally 7 at. % Fe content provided an independent value of 7.8 at. % Fe for this film. After deposition, the films were patterned into a six-terminal Hall-bar geometry. Measurements of the anomalous Hall effect at temperatures between 2 and 300 K provided the magnetization $M(T)$, from which the Curie temperatures of the films were deduced.

III. THEORETICAL APPROACH

A. Ground-state calculations

Within the present work, spin-polarized electronic-structure calculations for the ground state have been performed using the multiple-scattering Korringa-Kohn-Rostoker (KKR) Green's-function method[25] in the scalar-relativistic approximation. The local spin-density approximation for density-functional theory was used with the parametrization for the exchange-correlation potential due to Vosko *et al.*[26] The potential was treated within the atomic sphere approximation with the radii of the spheres around Fe/Co and Pd/Pt sites chosen by requiring the ratios of the corresponding volumes to be the same as for the pure elements. For the angular momentum expansion of the Green's function a cutoff of $l_{max}=3$ was applied. For substitutionally disordered alloys, the self-consistent coherent-potential approximation (CPA) method was employed. A geometry optimization was performed, i.e., the lattice constants of the alloys have been obtained by minimization of the total energy.

B. Extended Heisenberg Hamiltonian

The finite-temperature properties of the investigated systems were studied by Monte Carlo simulations based on the Heisenberg model with the underlying Hamiltonian given by

$$H_{ex} = -\sum_{ij} \tilde{J}_{ij}^{M\text{-}M} \vec{M}_i \vec{M}_j - \sum_{ij} \tilde{J}_{ij}^{M\text{-}m} \vec{M}_i \vec{m}_j - \sum_{ij} \tilde{J}_{ij}^{m\text{-}m} \vec{m}_i \vec{m}_j. \tag{1}$$

Here the classical Hamiltonian was generalized to allow an application to itinerant-electron systems consisting of magnetic and nonmagnetic atoms having magnetic moments M_i and m_i, respectively, connected with corresponding exchange coupling parameters. The dependence of the induced magnetic moments m_i on a specific magnetic configuration is treated via linear-response formalism (for details see the Appendix).

We suppose that the induced magnetic moments on Pd or Pt atoms are governed only by the magnetic moments of the Fe or Co atoms in Fe_xPd_{1-x} and Co_xPt_{1-x} alloys, respectively, arranged in the first-neighbor shell around the nonmagnetic atom so that

$$\vec{m}_i = \sum_{M_j \in \{M\}_1} X_{ij}^{m\text{-}M} \vec{M}_j = X_i^{m\text{-}M} \sum_{M_j \in \{M\}_1} \vec{M}_j. \tag{2}$$

The notation $\Sigma_{M_j \in \{M\}_1}$ means that the sum includes only such terms where j indicates a site with an inducing magnetic moment within the first-neighbor shell around the nonmagnetic atom i.

In this case (see the Appendix) the susceptibility $X_{ij}^{m\text{-}M}$ can be approximated by the value found for the ground state of a system with well defined collinear spontaneous (Fe, Co) and induced (Pd, Pt) magnetic moments,

$$X_i^{m\text{-}M} = \frac{m_i}{\sum_{M_j \in \{M\}_1}}. \tag{3}$$

The exchange coupling parameters $\tilde{J}_{ij}$ between atoms i and j in Eq. (1) were obtained via the formula of Lichtenstein *et al.*,[3]

$$J_{ij} = -\frac{1}{4\pi}\mathrm{Im}\int^{E_F} dE\ \mathrm{Tr}(t_{i\uparrow}^{-1} - t_{i\downarrow}^{-1})\tau_{\uparrow}^{ij}(t_{j\uparrow}^{-1} - t_{j\downarrow}^{-1})\tau_{\downarrow}^{ji} \tag{4}$$

with the relation

$$\tilde{J}_{ij} = \frac{J_{ij}}{|\vec{m}_i||\vec{m}_j|}. \tag{5}$$

In Eq. (4), $t_{i\sigma}$ and τ_{σ}^{ij} are the spin (σ) and site (i,j)-dependent single-site and scattering path operator matrices occurring within the KKR formalism.[27]

C. Evaluation of T_C

The Curie temperature T_C was evaluated with the MC method[28] using the standard Metropolis importance sampling algorithm[29] on the basis of the model Hamiltonian in Eq. (1). The number of atoms in the MC unit cell for different concentrations was taken between 1728 and 4000 and T_C was determined from the peak position of the temperature-dependent susceptibility. The Fe/Co magnetic moments were treated during MC simulation as localized and changing only their orientation. On the other hand, the magnetic moments on Pd/Pt atoms could change their absolute value as well as the orientation in accordance with the changing magnetic configuration around these atoms. Equation (2) implies that the magnetic moments on Pd/Pt are proportional to the vector sum of magnetic moments at neighboring Fe/Co atoms with only nearest neighbors taken into account. This means that each MC step consists of (1) change in the orientation of a magnetic moment on the Fe/Co atoms, and (2) search for all nearest-neighbor Pd/Pt atoms and calculation of the orientation and absolute value of their moments using the susceptibilities $X^{m\text{-}M}$ via Eq. (3). The change in the energy of the whole system is due to both effects. For disordered alloys the resulting T_C values in addition were averaged over up to 20 different configurations.

Obviously, the approach described above accounts for the contribution of spin-polarized nonmagnetic atoms to the exchange interactions between the magnetic atoms. As this contribution is temperature dependent, it allows a corresponding description of the temperature-dependent magnetization. In particular, it accounts for longitudinal spin fluctuations occurring on the nonmagnetic sublattice. It will be shown below that this rather simple scheme gives rather good agreement with experimental data for the systems under consideration.

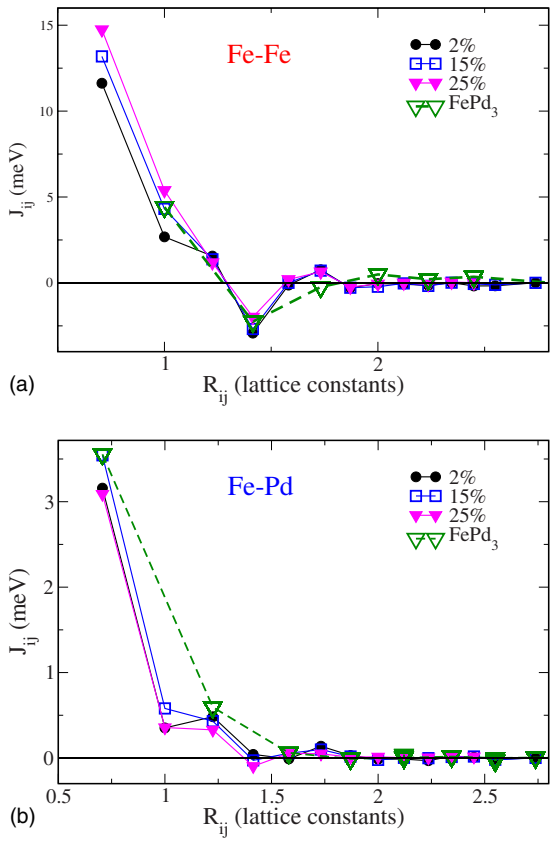

FIG. 1. (Color online) Exchange coupling parameters $J^{\text{Fe-Fe}}$ (a) and $J^{\text{Fe-Pd}}$ (b) for Fe_xPd_{1-x} alloys at different concentrations. The dashed lines represent results for ordered $FePd_3$ (note that in this case for the Fe atoms the nearest-neighbor interaction $J^{\text{Fe-Fe}}$ is absent because there are only Pd nearest neighbors).

IV. RESULTS FOR Fe_xPd_{1-x} ALLOYS

A. *Ab initio* calculations

The scheme for calculation of temperature-dependent magnetic properties, described above, was used to investigate disordered Fe_xPd_{1-x} alloys with Fe concentration up to 20 at. %. The exchange coupling parameters $J_{ij}^{\text{Fe-Fe}}$ and $J_{ij}^{\text{Fe-Pd}}$ shown in Fig. 1 have a similar dependency on the distance R_{ij} for all investigated alloys. In the Pd-rich limit (Fe concentration $x<0.2$) the exchange coupling parameters $J_{ij}^{\text{Fe-Fe}}$ corresponding to the average distance between magnetic atoms are rather small and do not allow to create long-range magnetic order in the system, as was demonstrated by corresponding restricted MC simulations. (An example of the snapshot magnetic-moment configuration at $T=0.1$ K for Fe_xPd_{1-x} alloy with Fe concentration 2 at. % is shown at Fig. 6.)

According to the experimental findings[30] the alloys exhibit ferromagnetic order for Fe concentrations above 0.1 at. %. In addition, previous experimental[31–38] and theoretical[15,39–43] investigations on the magnetic properties of Fe_xPd_{1-x} alloys have shown a strong host polarization by magnetic Fe impurities leading to a giant magnetic moment per impurity atom up to 12.9 μ_B. A widespread regime of magnetized Pd atoms leads to ferromagnetic order in diluted

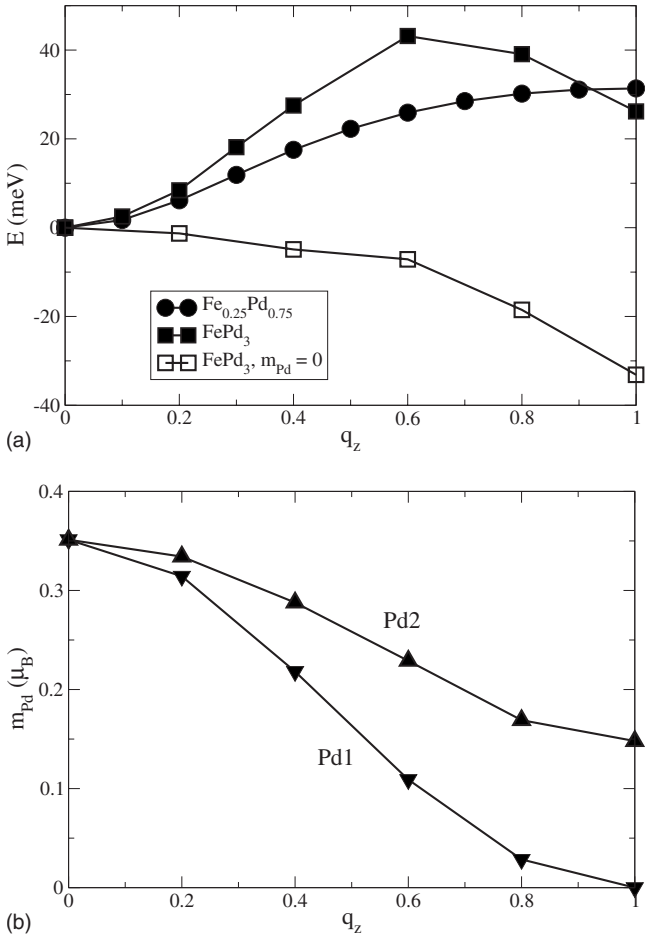

FIG. 2. Results of spin-spiral calculations for ordered $FePd_3$ and disordered $Fe_{0.25}Pd_{0.75}$: (a) the energy of spin spirals as a function of the wave vector $q=\frac{\pi}{a}(0,0,q_z)$, obtained for the disordered alloy (full circles), for the ordered compound with nonzero Pd magnetic moments (full squares), and for the ordered compound with Pd magnetic moments forced to be zero (open squares); (b) magnetic moment of inequivalent Pd atoms in ordered $FePd_3$ as a function of the wave vector q_z. Fe and Pd2 atoms occupy the sites (0,0,0) and $(\frac{1}{2},\frac{1}{2},0)$, respectively, Pd1 atoms occupy the sites $(0,\frac{1}{2},\frac{1}{2})$ and $(\frac{1}{2},0,\frac{1}{2})$.

Fe_xPd_{1-x} alloys despite a large distance between the magnetic Fe atoms.

The crucial role of the induced magnetic moment on Pd for the Fe-Fe exchange interactions can be demonstrated by an analysis of the energy of spin spirals given as a function of the wave vector. This is shown in Fig. 2 for the disordered alloy $Fe_{0.25}Pd_{0.75}$ in comparison with the results for the ordered compound $FePd_3$. The calculations have been performed for spin spirals along the z direction with the Fe magnetic moments tilted by 90° with respect to the z axis. For the ordered system an increase in the wave vector of the spin spirals is accompanied first by an increase in energy reflecting the stability of the ferromagnetic order in the system. A further increase in the wave vector above $q_z > \pi/2a$ leads to a decrease in the energy of the spin spiral [Fig. 2(a)]. This behavior is governed by a decrease in the Pd magnetic moments at these wave vectors [see Fig. 2(b)] that diminishes their role in the Fe-Fe exchange.

The role of Pd becomes clearly visible for the spin spirals in $FePd_3$ with the Fe-Pd exchange interactions being suppressed. This can be achieved by forcing the Pd-induced magnetic moments to be perpendicular to the Fe magnetic moments, and therefore to be equal to 0 (see the Appendix). In this case the minimum of the spin-spiral energy corresponds to an AFM state, i.e., at $q=\pi/a$ that originates from Fe-Fe exchange interaction (see Fig. 1). In the case of the disordered alloy the dependence of the spin-spiral energy on the wave vector is different because the random distribution of the Fe atoms allows Fe atoms to be nearest neighbors with a strong FM interaction. Due to this, the system retains the FM order at all values of the wave vector $\vec{q}$.

While the ground-state magnetic properties of Fe_xPd_{1-x} alloys can essentially be understood on the basis of *ab initio* electronic-structure calculations, a theoretical description of finite-temperature properties faces many difficulties due to the itinerant-electron nature of magnetism. Theoretical investigations based on the results of *ab initio* electronic-structure calculations have been performed, for example, by Mohn and Schwarz.[15] They used the model approach formulated by Bloch *et al.*[44] to describe the magnetic behavior of a system characterized by the coexistent local- and itinerant-electron magnetism. Within this approach the system is characterized by two interacting subsystems: (i) one having local magnetic moments showing a Curie-Weiss-type behavior and (ii) an itinerant electron subsystem magnetically polarized by the effective Weiss field with the corresponding parameters found by *ab initio* electronic-structure calculations.

The spin moment on every Pd atom is induced by the magnetic moment of the Fe atoms and all surrounding induced Pd magnetic moments (see the Appendix). The fact that the magnetic moment induced in Pd is rather large and that the region of nonzero Pd magnetization spreads to large distances from the inducing Fe atom is a result of the high magnetic spin susceptibility of pure Pd as well as Fe_xPd_{1-x} alloys with small Fe concentration. This is determined by a large Pd density of states (DOS) at the Fermi level $n(E_F)$ [see Fig. 3(a)]. In turn, $n(E_F)$ decreases with the increase in Fe content in the alloy [Fig. 3(b)], resulting in a decrease in the partial magnetic susceptibility of the Pd atoms. Thus, at very small Fe concentrations the induced Pd spin moment can extend to big distances by inducing shell by shell a spin moment in the Pd subsystem. This polarization mechanism decays with the distance from the magnetic impurity. When the Fe concentration increases the regions with the induced moments overlap. As was pointed in Shimizu *et al.*,[45,46] when the Fe concentration is larger than 0.1 at. % the Pd magnetic properties can be described well by band calculations, as done in our present work using the CPA alloy theory.

Figures 3(c) and 3(d) represent the spin magnetic moments of Pd and Fe versus the Fe content in Fe_xPd_{1-x}. As can be seen, the Fe magnetic moments change only slowly with the increase in Fe concentration while the variation in the Pd spin magnetic moments is rather pronounced. This can be directly connected to the decrease in the Pd DOS at the Fermi level.

For a more detailed analysis we investigated the properties of the induced Pd magnetic moment using the *ab initio*

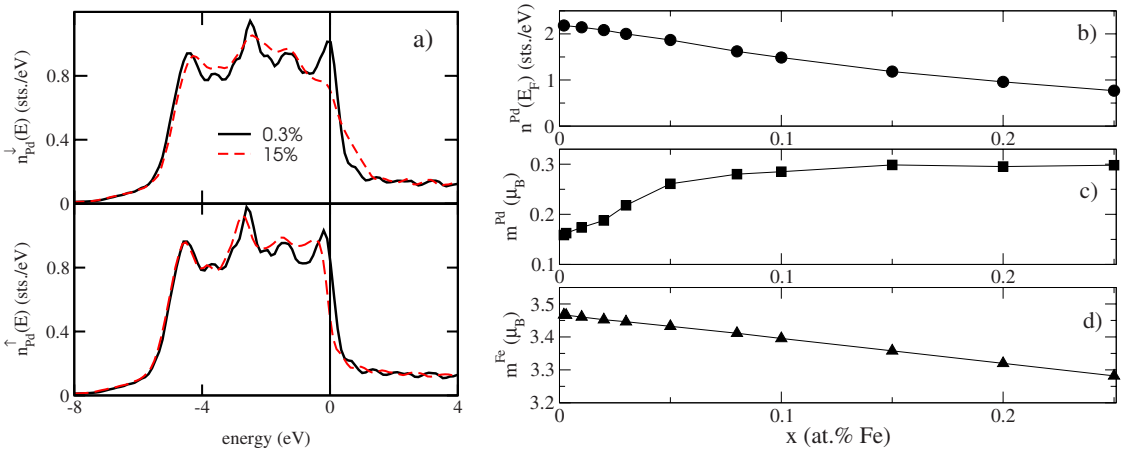

FIG. 3. (Color online) (a) Pd DOS in Fe_xPd_{1-x} for $x=0.003$ and $x=0.15$ for spin-down (upper panel) and spin-up (lower panel) states. Ground-state characteristics of Fe_xPd_{1-x} alloys vs Fe concentration; (b) density of states of Pd at the Fermi level; (c) Pd spin magnetic moments; and (d) Fe spin magnetic moments.

calculations. In particular, we studied the distribution of the Pd magnetic moment in a Pd host in the limit of very small Fe concentrations, i.e., around a single Fe impurity. To see that the induced magnetic moment at every Pd atom is determined not only by the Fe magnetic moment but also by the surrounding Pd magnetic moments, one can compare the unenhanced induced Pd spin moments created by only one Fe atom with the total induced spin moments in Pd. The total induced magnetic-moment distribution in Pd can be found by solving the system of Eq. (A3) within a selected region around an Fe atom (see the Appendix). In addition, in the present work the moment distribution has been obtained by self-consistent electronic-structure calculations instead of using linear-response formalism. Figure 4 shows the slow decay of the induced magnetic moment with the distance (full squares). The corresponding unenhanced induced moment in these calculations has been obtained by suppressing the effective exchange B field in the Pd atoms during the SCF cycle. These unenhanced magnetic moments (closed circles) compare very well with those obtained from linear-response formalism [Eq. (A1)] (open circles). These are shown in Fig. 4 also for larger distances. One can see that the decrease with the distance of the Pd unenhanced spin moment is very fast compared to the enhanced one. For the nearest Pd neighbors of Fe atom these values differ approximately by a factor of 2 while the difference for the next-nearest neighbors is already an order of magnitude. The local exchange enhancement, well approximated within the linear approach at small values of the induced magnetic moments, should keep the ratio of these two values approximately constant. The obtained results give evidence for a more complicated picture of the creation of the induced magnetic moment in accordance to the description given in the Appendix.

The effect of temperature-induced magnetic disorder within the Fe subsystem was analyzed within *ab initio* calculations, describing magnetic disorder within the uncompensated disordered local moment (DLM) approximation. Using this approximation an effective alloy of two types of Fe atoms with opposite spin directions and having different concentrations is treated using the CPA alloy theory. In this way one can study the dependence of the induced magnetic moment of individual Pd atoms on the average magnetic moment in the system. Figure 5 shows that the magnetic disorder in the Fe subsystem (assumed to be temperature induced), accompanied by a decrease in the average Fe magnetic moment $\langle m_{Fe}\rangle$, results in a decrease in the induced magnetic moment in the Pd subsystem. One can see a rather good linear dependence of the induced Pd magnetic moment as a function of the magnetic moment of the Fe subsystem, for nearly all Fe concentrations. Only in the limiting case of low Fe concentration (1 at. %), a noteworthy deviation from linear behavior is observed. This deviation will influence the final results in a Curie temperature evaluation correspondingly.

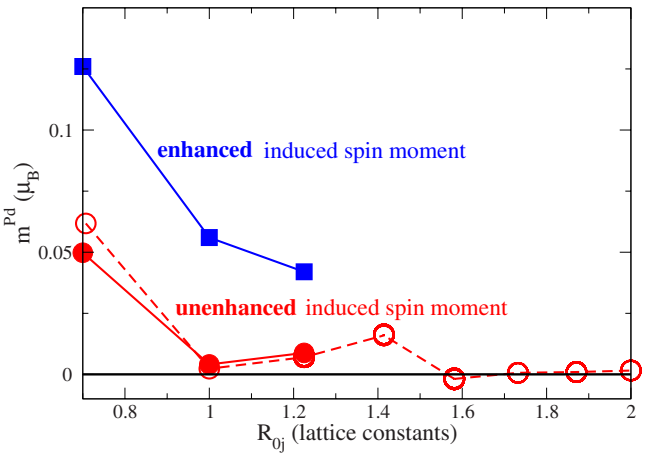

FIG. 4. (Color online) Magnetic moment distribution in Pd around a single Fe impurity, as a function of the distance from the magnetic atom. Full squares represent the Pd magnetic moments self-consistently obtained within a cluster with three atomic shells of Pd around an Fe impurity embedded into a Pd host and full circles give the results obtained for the same system but with the exchange potential switched off. The open circles represent the induced magnetic moments in Pd calculated within linear-response formalism using Eq. (A1) in the Appendix.

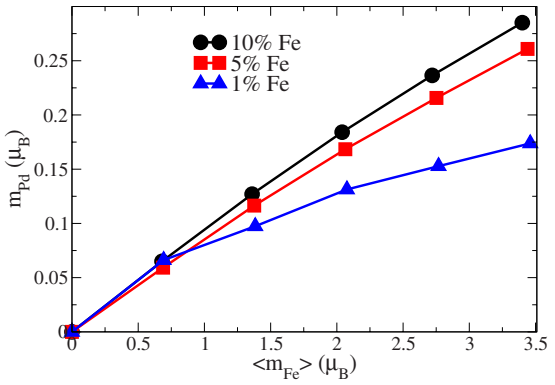

FIG. 5. (Color online) Results of *ab initio* calculations by using the uncompensated DLM approximation: induced Pd moment in three Fe-Pd alloys as a function of the Fe average magnetic moment.

B. Finite-temperature magnetism of Fe_xPd_{1-x} alloys

The temperature-dependent magnetic properties of Fe_xPd_{1-x} alloys were investigated by performing Monte Carlo simulations. They show an absence of an ordered FM state for the alloys with Fe concentration up to $x \approx 0.2$ if the Fe-Fe exchange interactions mediated by Fe-Pd interactions are neglected. This clearly demonstrates the importance of these interactions. For disordered $Fe_{0.2}Pd_{0.8}$ alloy the FM order can be obtained despite neglecting the Pd-mediated Fe-Fe interactions. However, the Curie temperature in this case is around 60 K, i.e., much lower than observed experimentally (around 400 K). To illustrate the role of Fe-Pd interactions in the formation of magnetic order, Fig. 6 shows spin configurations obtained within MC simulations at $T=0.1$ K for the Fe_xPd_{1-x} alloy with $x=0.02$ for one particular distribution of Fe atoms. Figure 6(a) represents a result for the case that the Fe-Pd exchange interactions are neglected and therefore it shows only the magnetic moments of Fe. As one can see, there is no magnetic order in the system because of weak Fe-Fe interaction at this Fe concentration. Figure 6(b) represents the spin configuration when the Fe-Pd first-neighbor interactions are taken into account and shows only those Fe and Pd magnetic moments which give a contribution to the total energy of a system given by Eq. (1). The FM order in this case is clearly seen.

A comparison of T_C for Fe_xPd_{1-x} alloys obtained within the MC simulation based on the Hamiltonian in Eq. (1) with the experimental data for Fe_xPd_{1-x} alloys is shown in Fig. 7. Obviously, a rather good agreement is obtained for the whole concentration range. It should be emphasized once more that all parameters for the model Hamiltonian [Eq. (1)] are obtained within *ab initio* electronic-structure calculations using the scheme described in the Appendix. Of course, going beyond the various approximations the final results can be improved to get better agreement with the experimental results. Figure 7 shows that the theoretical results obtained by Mohn and Schwarz[15] for Fe_xPd_{1-x} alloys at small Fe concentrations are also in a good agreement with experiment. However, it should be emphasized that this latter work is based on a semiphenomenological approach.

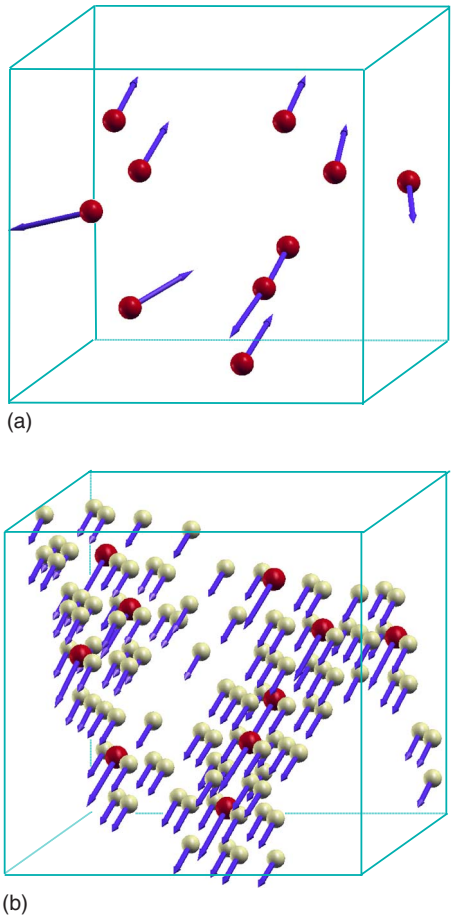

FIG. 6. (Color online) Fe_xPd_{1-x} alloy with 2 at. % Fe: the magnetic moment snapshot configuration in a unit cell used within the MC simulations ($T=0.1$ K) (a) without and (b) with the induced Pd moments taken into account. Large arrows correspond to the Fe magnetic moments and small arrows to Pd magnetic moments.

V. RESULTS FOR Co_xPt_{1-x} ALLOYS

A. Magnetic moments and exchange coupling constants

The calculated equilibrium lattice constants for ordered and disordered Co_xPt_{1-x} alloys are shown in Table I. For

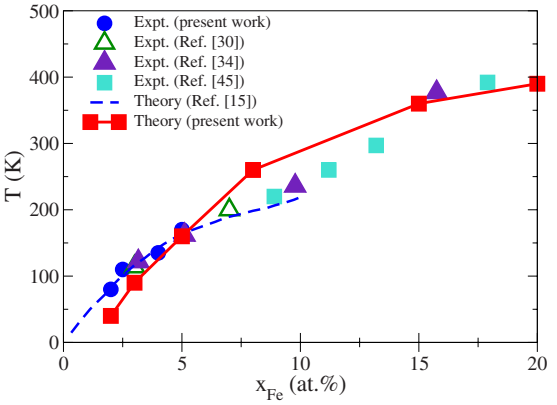

FIG. 7. (Color online) The Curie temperature for different Fe concentrations in Fe_xPd_{1-x} alloys: present results vs theoretical results of Mohn and Schwarz (Ref. 15) and experimental data.

TABLE I. Equilibrium lattice constants and magnetic moments at Co and Pt atoms for ordered and disordered Co_xPt_{1-x} alloys.

System		a (a.u.)	μ_{spin} (Co) (μ_B)	μ_{spin} (Pt) (μ_B)
Co_3Pt	Ordered	6.98	1.82	0.36
	Disordered	7.06	1.88	0.25
CoPt	Ordered	7.23	1.93	0.37
	Disordered	7.23	2.03	0.27
$CoPt_3$	Ordered	7.31	1.76	0.26
	Disordered	7.37	2.19	0.25

ordered CoPt we used a simplified $L1_0$ geometry assuming $c=a$ instead of $c=0.98a$ found in experiment. The magnetic moments of the Co and Pt atoms for the equilibrium lattice constants obtained in the scalar-relativistic mode are presented in Table I. More details about ground-state properties of Co-Pt can be found in our earlier study.[47]

The exchange coupling constants J_{ij} for the investigated systems were evaluated via Eq. (4). The dependence of J_{ij} on the distance between the atoms i and j is displayed in Fig. 8 with the left panels showing the situation when both i and j are Co atoms and the right panels showing the situation when i is a Co atom and j is a Pt atom. If experimental lattice constants were used instead of equilibrium lattice constants, the J_{ij} constants would change slightly but both the trends and the values would remain similar as in Fig. 8.

One can see from Fig. 8 that for Co_3Pt and CoPt the coupling between the moments on the Co atoms do not differ very much from the results for their disordered counterparts, $Co_{0.75}Pt_{0.25}$ and $Co_{0.50}Pt_{0.50}$, respectively. However, the situation changes dramatically for $CoPt_3$ (lower left panel in Fig. 8). The pronounced difference between the data for the ordered and the disordered system stems mainly from the fact that there are no Co atoms present for some coordination spheres around a central Co atom in ordered $CoPt_3$. Concerning the coupling between moments on Co and Pt atoms, the degree of long-range order has a larger influence than for the Co-Co coupling. For ordered alloys, the J_{ij} constants significantly vary also with composition. For disordered alloys, on the other hand, the J_{ij} constants do not vary very much with composition. For ordered $CoPt_3$, there is a surprisingly strong Co-Co coupling between atoms which are $2.83a$ apart. We verified that for larger distances no comparable strong coupling occurs.

B. Curie temperatures

The Curie temperatures T_C of the investigated Co-Pt systems evaluated by means of the Monte Carlo technique are shown in Table II. In addition, results for fcc Co are given in this table. The two theoretical Curie temperatures correspond to two different Hamiltonians used to describe the magnetic coupling. The first T_C (denoted as "Co-Co only" in Table II) corresponds to the standard Heisenberg Hamiltonian for magnetic moments only on the Co atoms. The second T_C (denoted as "Co-Co and Co-Pt") corresponds to the extended Heisenberg Hamiltonian [Eq. (1)], accounting for the coupling between moments on Co atoms $\tilde{J}_{ij}^{\text{Co-Co}}$ as well as for the coupling between moments on Co and Pt atoms $\tilde{J}_{ij}^{\text{Co-Pt}}$, with the moments on Pt atoms determined via Eqs. (2) and (3). The values of T_C obtained earlier by relying on the semiempirical Mohn-Wohlfarth theory[52] were taken from Qi *et al.*[50] for fcc Co, from Kashyap *et al.*[22] for ordered Co-Pt compounds, and from Ghosh *et al.*[51] for disordered Co_xPt_{1-x} alloys. Experimental values[48,49] are shown for comparison. Note that an experimental value for T_C for ordered Co_3Pt is not available because the ordered phase is not stable for this composition.

TABLE II. Curie temperatures T_C for fcc Co and for ordered and disordered Co_xPt_{1-x} alloys. Experimental results (Refs. 48 and 49) are shown together with the results of our Monte Carlo calculations with either both Co-Co and Co-Pt coupling or with only Co-Co coupling included. For comparison, results obtained by relying on the Mohn-Wohlfarth theory are also shown (Refs. 22, 50, and 51). Negative T_C implies antiferromagnetic ordering.

System	Model	T_C ordered (K)	T_C disordered (K)
fcc Co	MC	1100	
	Experiment	1388	
	Mohn-Wohlfarth	3523	
Co_3Pt	MC, Co-Co only	800	750
	MC, Co-Co and Co-Pt	900	880
	Experiment		1100
	Mohn-Wohlfarth	1803	1120
CoPt	MC, Co-Co only	360	620
	MC, Co-Co and Co-Pt	620	760
	Experiment	727	830
	Mohn-Wohlfarth	1964	850
$CoPt_3$	MC, Co-Co only	−180	370
	MC, Co-Co and Co-Pt	150	520
	Experiment	288	468
	Mohn-Wohlfarth	241	510

As can be seen, the Mohn-Wohlfarth theory[52] gives reasonable agreement with experiment at small Co concentration. However, increasing the Co content leads to large discrepancies between the theory and experiment. This results from the limitations of the Mohn-Wohlfarth theory: it was developed for homogeneous itinerant-electron systems, which is not the case for Co_xPt_{1-x} alloys.

Our *ab initio* scheme based on an extended Heisenberg Hamiltonian (both Co-Co and Co-Pt coupling included) accounts quantitatively for the trends of T_C with the composition and with the degree of long-range order. If the coupling mediated via moments at Pt atoms is not included, the results are unrealistic. This is especially true for ordered $CoPt_3$, where an *antiferromagnetic* order is established at finite temperatures (reflected by a negative value for T_C) if the coupling between moments on Co and Pt is ignored.

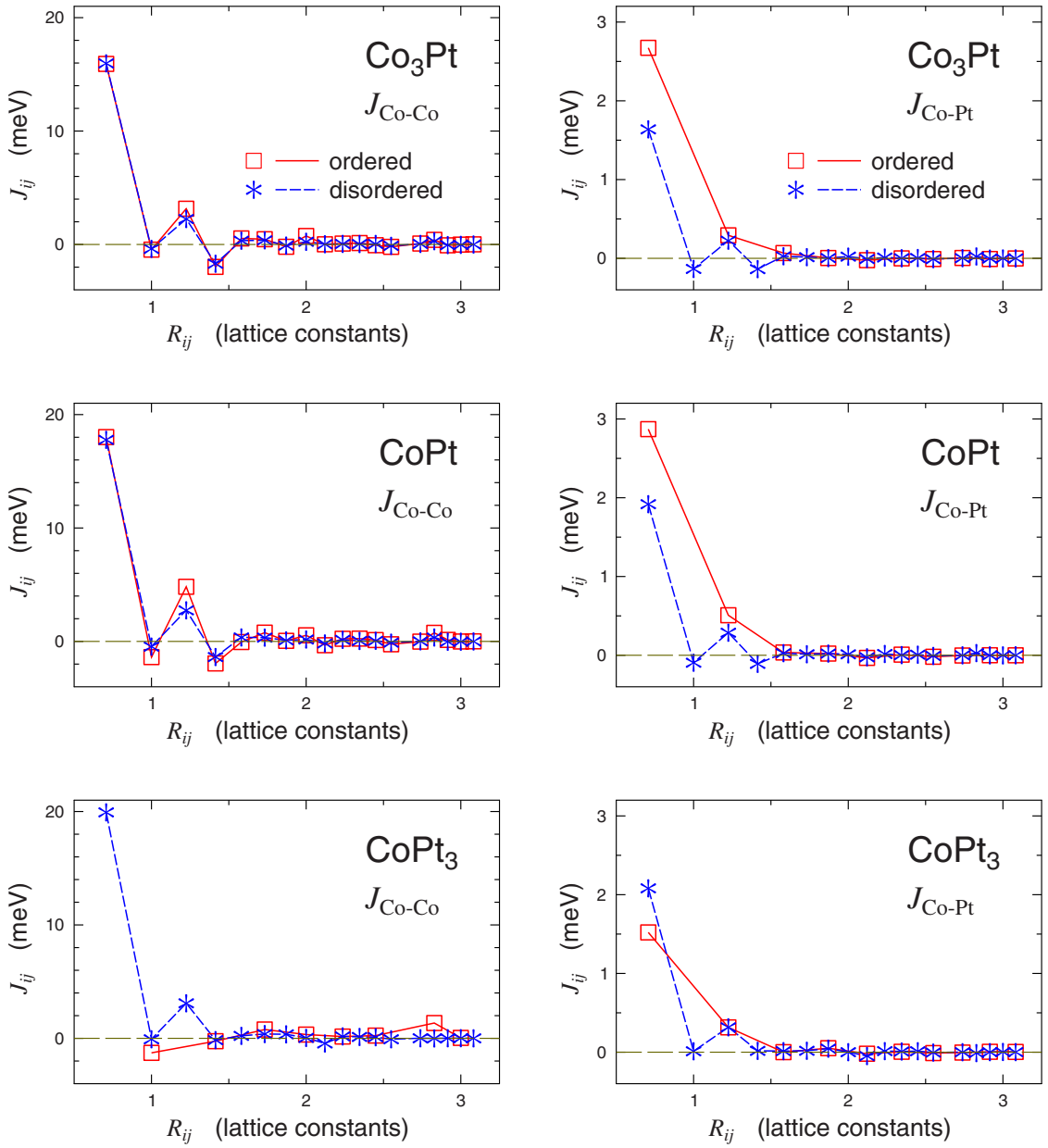

FIG. 8. (Color online) Exchange coupling constants J_{ij} between moments of Co atom on site i and on other surrounding Co atoms (j) (left panels) and between moments on Co atom (i) and on surrounding Pt atoms (j) (right panel), for ordered and disordered Co_xPt_{1-x} alloys. The horizontal axis shows the distance R_{ij} between i and j atoms in units of lattice constants.

VI. CONCLUSIONS

As was shown in the present work by the examples of Fe_xPd_{1-x} and Co_xPt_{1-x} alloys, the finite-temperature magnetism of alloys composed of magnetic and nonmagnetic elements requires to account for the exchange interactions between magnetic atoms, mediated by the exchange interaction with nonmagnetic atoms. This implies, in particular, that one has to account properly for the induced magnetic moment within the Monte Carlo simulations which are based in the present work on a corresponding extension of the standard Heisenberg Hamiltonian. The approach presented suggests to describe the induced magnetic moment on nonmagnetic atoms within linear-response formalism, being proportional to the vector sum of magnetic moments of neighboring magnetic atoms. This ansatz allows for substantial technical simplifications and leads to substantial improvement of the results when compared to simpler schemes.

The finite-temperature calculations for Fe_xPd_{1-x} and Co_xPt_{1-x} alloys performed within this approach give the dependence of T_C on the composition as well as on the degree of long-range order in good agreement with experimental data. The case of ordered $CoPt_3$ also demonstrates that even if the coupling between nearest inducing moments is antiferromagnetic, the magnetic order can still be ferromagnetic due to the effect of coupling between inducing and induced moments. A mere inspection of the J_{ij} constants thus cannot

serve as a reliable indicator of ferromagnetic or antiferromagnetic order at $T \neq 0$ K.

ACKNOWLEDGMENTS

This work was supported by the DFG within the SFB 689 "Spinphänomene in reduzierten Dimensionen" as well as the project Eb 154/20 "Spin polarisation in Heusler alloy based spintronics systems probed by SPINAXPES," and by GA CR within the Project No. 202/08/0106.

APPENDIX: INDUCED MAGNETIC MOMENTS

The magnetic moment induced on site i (Pd or Pt) by the exchange field $\vec{B}_j^{xc}$ due to magnetic moments at site j can be calculated within the linear-response formalism using the expression,[53]

$$\vec{m}_i^0(\vec{r}) = -\frac{1}{\pi}\mathrm{Im}\int^{E_F} dE\ \mathrm{Tr}\ \vec{\sigma} \times \int_{\Omega_j} d^3r' G(\vec{r},\vec{r}',E) H_j^{xc}(\vec{r}') G(\vec{r}',\vec{r},E) = \int_{\Omega_j} \chi_{ij}(\vec{r},\vec{r}')\vec{B}_j^{xc}(r')d^3r'. \quad \text{(A1)}$$

Here $H_j^{xc}(\vec{r}') = \vec{\sigma}\vec{B}_j^{xc}(\vec{r}') = \vec{\sigma}\vec{e}_M B_j^{xc}(\vec{r}')$ with $\vec{\sigma}$ the matrix of Pauli matrices,[54] $\vec{e}_M$ the unit vector in the direction of spontaneous magnetic moment of atom j, and $B_j^{xc}(\vec{r})$ the local exchange field at the site j. Note that neglecting relativistic effects, the magnetic moment $\vec{m}_i^0$ induced by a neighboring magnetic atom is parallel to the direction $\vec{e}_M$ of the magnetic moment $\vec{M}_j$ of this atom.

The total induced magnetic moments on a Pd or Pt atom is represented as a response to the exchange field of all surrounding atoms by the following expression:

$$\vec{m}_i(\vec{r}) = \sum_{j\in M}\int_{\Omega_j^M} \chi_{ij}^{m\text{-}M}(\vec{r},\vec{r}')\vec{B}_j^{xc,M}(\vec{r}')d^3r' + \sum_{j\in m}\int_{\Omega_j^m} \chi_{ij}^{m\text{-}m}(\vec{r},\vec{r}')\vec{B}_j^{xc,m}(\vec{r}')d^3r' + \chi_i^0(\vec{r})\vec{B}_i^{xc,m}(\vec{r}). \quad \text{(A2)}$$

Analogous to $\Sigma_{j\in M}$ defined at Eq. (2), the sum $\Sigma_{j\in m}$ means summation over sites with induced magnetic moments.

This can be reformulated in terms of local magnetic moments M_i of Fe (Co) and m_i of Pd (Pt)

$$m_i = \sum_{j\in M}\tilde{\chi}_{ij}^{m\text{-}M}\vec{M}_j + \sum_{j\in m}\tilde{\chi}_{ij}^{n\text{-}m}\vec{m}_j + \tilde{\chi}_{ii}\vec{m}_i \quad \text{(A3)}$$

with

$$\vec{M}_i = \int_{\Omega_{WS}} d^3r\vec{M}_i(\vec{r}), \quad \vec{m}_i = \int_{\Omega_{WS}} d^3r\vec{m}_i(\vec{r}). \quad \text{(A4)}$$

Here we use the following reformulation for the first term in Eq. (A2) that is more convenient for the model implementation:

$$\int_{\Omega_j^M}\chi_{ij}^{m\text{-}M}(r,r')\vec{B}_j^{xc,M}(r')d^3rd^3r' = \vec{M}_j\int_{\Omega_j^M}\chi_{ij}^{m\text{-}M}(r,r')\frac{B_j^{xc,M}(r')}{M_j}d^3rd^3r' = \tilde{\chi}_{ij}^{m\text{-}M}\vec{M}_j. \quad \text{(A5)}$$

For the second term, using a linearized expression for the exchange potential in the case of a small induced magnetic moment on Pd and Pt sites,[53,55] one can write analogously,

$$\int_{\Omega_j^m}\chi_{ij}^{m\text{-}m}(r,r')\vec{B}_j^{xc,m}(r')d^3rd^3r' = \vec{m}_j\int_{\Omega_j^m}\chi_{ij}^{m\text{-}m}(r,r')\left.\frac{\delta V_j^{xc}[n,m]}{\delta m(\vec{r})}\right|_{m=0}\frac{m_j(\vec{r})}{m_j}d^3rd^3r' = \tilde{\chi}_{ij}^{m\text{-}m}\vec{m}_j. \quad \text{(A6)}$$

Solving the system of Eq. (A3) for a restricted region around a magnetic impurity atom gives the distribution of the induced magnetic moments on the nonmagnetic atoms. This can be done for the ground state ($T=0$ K). Alternatively, without any approximations, one can get these values within *ab initio* calculations for embedded magnetic atoms by using the CPA alloy theory, assuming a uniform distribution of the induced magnetic moment.

Strictly spoken, one can go beyond the linear approximation in the expansion of the exchange potential. However, the linear approximation makes the use of this scheme in subsequent Monte Carlo simulations much easier.

By making an additional simplification one can restrict to one response function $X_{ij}^{m\text{-}M}$ within the Monte Carlo simulations. This quantity is defined to give the induced magnetic moment as a response to the exchange fields of only the surrounding nearest-neighbor magnetic atoms,

$$\vec{m}_i = \sum_{j\in M} X_{ij}^{m\text{-}M}\vec{M}_j. \quad \text{(A7)}$$

Substituting this equation into Eq. (A3) we can obtain an expression for $X_{ij}^{m\text{-}M}$ which shows explicitly an enhancement of the direct response function $\tilde{\chi}_{ij}^{m\text{-}M}$ [the first term in Eq. (A3)] caused by the induced magnetic moments at nonmagnetic atoms,

$$X_{ij}^{m\text{-}M} = \frac{\tilde{\chi}_{ij}^{m\text{-}M}}{1-\sum_{j\in m}\tilde{\chi}_{ij}^{m\text{-}m}-\tilde{\chi}_{ii}}. \quad \text{(A8)}$$

[1] J. Kübler, *Theory of Itinerant Electron Magnetism* (Oxford University Press, Oxford, 2000), p. 460.
[2] P. Mohn, *Magnetism in the Solid State* (Springer, Berlin, 2003), p. 215.
[3] A. I. Liechtenstein, M. I. Katsnelson, V. P. Antropov, and V. A. Gubanov, J. Magn. Magn. Mater. **67**, 65 (1987).
[4] G. Fischer, M. Däne, A. Ernst, P. Bruno, M. Lüders, Z. Szotek, W. Temmerman, and W. Hergert, Phys. Rev. B **80**, 014408 (2009).
[5] T. Fukushima, K. Sato, H. Katayama-Yoshida, and P. H. Dederichs, Jpn. J. Appl. Phys., Part 2 **43**, L1416 (2004).
[6] I. Turek, J. Kudrnovský, V. Drchal, P. Bruno, and S. Blügel, Phys. Status Solidi B **236**, 318 (2003).
[7] J. Hubbard, Phys. Rev. B **19**, 2626 (1979).
[8] T. Moriya, *Spin Fluctuations in Itinerant Electron Magnetism* (Springer, Berlin, 1985).
[9] H. Hasegawa, J. Phys. Soc. Jpn. **46**, 1504 (1979).
[10] V. Korenman, J. L. Murray, and R. E. Prange, Phys. Rev. B **16**, 4032 (1977).
[11] M. Uhl and J. Kübler, Phys. Rev. Lett. **77**, 334 (1996).
[12] N. M. Rosengaard and B. Johansson, Phys. Rev. B **55**, 14975 (1997).
[13] A. V. Ruban, S. Khmelevskyi, P. Mohn, and B. Johansson, Phys. Rev. B **75**, 054402 (2007).
[14] A. R. Williams, R. Zeller, V. L. Moruzzi, C. D. Gelatt, and J. Kubler, J. Appl. Phys. **52**, 2067 (1981).
[15] P. Mohn and K. Schwarz, J. Phys.: Condens. Matter **5**, 5099 (1993).
[16] O. N. Mryasov, U. Nowak, K. Y. Guslienko, and R. W. Chantrell, Europhys. Lett. **69**, 805 (2005).
[17] O. N. Mryasov, Phase Transitions **78**, 197 (2005).
[18] M. Ležaic, P. Mavropoulos, J. Enkovaara, G. Bihlmayer, and S. Blügel, Phys. Rev. Lett. **97**, 026404 (2006).
[19] L. M. Sandratskii, R. Singer, and E. Şaşioğlu, Phys. Rev. B **76**, 184406 (2007).
[20] J. A. Christodoulides, Y. Huang, Y. Zhang, G. C. Hadjipanayis, I. Panagiotopoulos, and D. Niarchos, J. Appl. Phys. **87**, 6938 (2000).
[21] G. Moulas, A. Lehnert, S. Rusponi, J. Zabloudil, C. Etz, S. Ouazi, M. Etzkorn, P. Bencok, P. Gambardella, P. Weinberger, and H. Brune, Phys. Rev. B **78**, 214424 (2008).
[22] A. Kashyap, K. B. Garg, A. K. Solanki, T. Nautiyal, and S. Auluck, Phys. Rev. B **60**, 2262 (1999).
[23] M. Schöck, C. Sürgers, and H. v. Löhneysen, Eur. Phys. J. B **14**, 1 (2000).
[24] W. Meindl, Ph.D. thesis, University of Regensburg, 2009.
[25] H. Ebert, in *Electronic Structure and Physical Properties of Solids*, Lecture Notes in Physics Vol. 535, edited by H. Dreyssé (Springer, Berlin, 2000), p. 191.
[26] S. H. Vosko, L. Wilk, and M. Nusair, Can. J. Phys. **58**, 1200 (1980).
[27] P. Weinberger, *Electron Scattering Theory for Ordered and Disordered Matter* (Oxford University Press, Oxford, 1990).
[28] K. Binder, Rep. Prog. Phys. **60**, 487 (1997).
[29] D. P. Landau and K. Binder, *A Guide to Monte Carlo Simulations in Statistical Physics* (Cambridge University Press, Cambridge, 2000).
[30] J. Crangle and W. R. Scott, J. Appl. Phys. **36**, 921 (1965).
[31] V. D. Gerstenberg, Ann. Phys. **457**, 236 (1958).
[32] J. W. Cable, E. O. Wollan, and W. C. Koehler, Phys. Rev. **138**, A755 (1965).
[33] P. P. Craig, B. Mozer, and S. Romeo, Phys. Rev. Lett. **14**, 895 (1965).
[34] G. Longworth, Phys. Rev. **172**, 572 (1968).
[35] G. Chouteau and R. Tournier, J. Phys. Colloq. **32**, C1-1002 (1971).
[36] J. Crangle, Philos. Mag. **5**, 335 (1960).
[37] B.-H. Yeh, J. Chen, P. K. Tseng, and S.-H. Fang, Chin. J. Phys. **13**, 1 (1975).
[38] J. F. van Acker *et al.*, Phys. Rev. B **38**, 10463 (1988).
[39] D.-K. Kim, Phys. Rev. **149**, 434 (1966).
[40] G. Bergmann, Phys. Rev. B **23**, 3805 (1981).
[41] R. Medina and R. E. Parra, J. Appl. Phys. **53**, 2201 (1982).
[42] Cai Jian-Wang, Luo He-Lie, Zeng Zhi, and Zheng Qing-Qi, J. Phys.: Condens. Matter **5**, 5343 (1993).
[43] A. Oswald, R. Zeller, and P. H. Dederichs, Phys. Rev. Lett. **56**, 1419 (1986).
[44] D. Bloch, D. M. Edwards, M. Shimizu, and J. Voiron, J. Phys. F: Met. Phys. **5**, 1217 (1975).
[45] T. Takahashi and M. Shimizu, J. Phys. Soc. Jpn. **20**, 26 (1965).
[46] M. Shimizu and T. Kato, Phys. Lett. **27A**, 166 (1968).
[47] O. Šipr, J. Minár, S. Mankovsky, and H. Ebert, Phys. Rev. B **78**, 144403 (2008).
[48] C. E. Dahmani, Ph.D. thesis, Louis Pasteur University, 1985.
[49] M. C. Cadeville, C. E. Dahmani, and F. Kern, J. Magn. Magn. Mater. **54-57**, 1055 (1986).
[50] Q. Qi, R. Skomski, and J. M. D. Coey, J. Phys.: Condens. Matter **6**, 3245 (1994).
[51] S. Ghosh, C. B. Chaudhuri, B. Sanyal, and A. Mookerjee, J. Magn. Magn. Mater. **234**, 100 (2001).
[52] P. Mohn and E. P. Wohlfarth, J. Phys. F: Met. Phys. **17**, 2421 (1987).
[53] M. Deng, H. Freyer, J. Voitländer, and H. Ebert, J. Phys.: Condens. Matter **13**, 8551 (2001).
[54] M. E. Rose, *Relativistic Electron Theory* (Wiley, New York, 1961).
[55] S. Mankovsky and H. Ebert, Phys. Rev. B **74**, 054414 (2006).